

THE BNL EBPM ELECTRONICS, HIGH PERFORMANCE FOR NEXT GENERATION STORAGE RINGS*

K. Vetter[#], Oak Ridge National Laboratory, Oak Ridge, TN, 37831, USA

J. Mead, B. Podobedov, Y. Tian, W. Cheng, Brookhaven National Laboratory, Upton, NY, USA

Abstract

A custom state-of-the-art RF BPM (EBPM) has been developed and commissioned at the Brookhaven National Laboratory (BNL) National Synchrotron Light Source II (NSLS-II). A collaboration between Lawrence Berkeley National Laboratory (LBNL) Advanced Light Source (ALS) and BNL has proven to be a key element in the success of the NSLS-II EBPM.

High stability coherent signal processing has allowed for demonstrated 200nm RMS spatial resolution and true turn-by-turn position measurement capability. Sub-micron 24 hr. stability has been demonstrated at NSLS-II by use of 0.01°C RMS thermal regulation of the electronics racks without the need of active pilot tone correction [1, 2].

The intentional partitioning during the conceptual architecture development phase of the RF and digital processing into separate boards has enabled rapid independent development of the analog front end board (AFE) and digital front end board (DFE). The partitioning of the AFE and DFE has realized derivative instrumentation platforms including the NSLS-II Cell Controller used for Fast Orbit Feedback SVD computation and corrector actuation, the NSLS-II photo-emission X-ray BPM. A CVD diamond beamline BPM (DBPM) based on the NSLS-II Xray BPM has been develop in conjunction with Sydor Technologies via an SBIR arrangement that has been implement on NSLS-II beamlines for local active beamline stabilization [3]. An MOU with LBNL was signed near the end of the NSLS-II EBPM development in which complete transfer of technology was provided as the basis of the LBNL ALS orbit upgrade.

INTRODUCTION

The development of the NSLS-II EBPM began in August of 2009. The development was primarily motivated in order to achieve world class performance using state-of-the-art technology with the ability of local BNL experts to optimize and evolve the EBPM.

Although funds were provided to support a development laboratory and personal, the NSLS-II project baseline was based on commercial EBPM technology. The criterion set to change the project baseline was to demonstrate to an expert external and internal review committee EBPM performance on an operational machine that sufficiently demonstrated compliance of the NSLS-II EBPM performance requirements, twelve months from the start of the development project.

A collaboration with ALS staff was quickly established

in which prototype NSLS-II EBPM beam tests would be conducted at ALS. The ALS machine was chosen as the optimal test facility as the machine RF frequency was close to NSLS-II and only required a change in the ADC sampling reference VCXO. The collaboration with the ALS staff quickly evolved into ALS staff making significant contributions to the physical design of the DFE FPGA design, which were extremely critical at the time do to the very aggressive proof-of-principal schedule that had been set. The first EBPM beam test at ALS was conducted in June of 2010, ten months after the start of the EBPM development.

Early tests were performed prior to the full development of the DFE and were structured to enable streaming of raw ADC data to file via Matlab TCP/IP connection. Capture of the raw ADC data in long data records (1Mpts or greater) allowed for detailed time and frequency analysis of the real world impairments imparted by the AFE. It was also possible to explore optimal processing algorithms with real-world impairments offline.

Rapid maturity of the EBPM AFE and DFE enabled detail studies at ALS demonstrating sub 200nm performance of 500mA dual-cam shaft user beam that served as the basis for the EBPM review committee to recommend changing the project baseline to include the custom NSLS-II EBPM.

EBPM DESIGN FOR SUB-MICRON PERFORMANCE

The design of and an EBPM for 3rd generation light sources and beyond is primarily composed of two aspects; spatial resolution, and stability. The first can be decomposed into turn-by-turn (TbT) and stored beam resolution.

User operation is typically concerned with stored beam resolution and stability, however, TbT measurements can be very useful for optimizing machine performance particularly at low bunch charge [4]. Achieving true TbT measurements is dependent on sufficient RF bandwidth to allow for the bunch energy to sufficiently decay within a single turn, and stringent coherent processing.

Stored beam spatial resolution is typically set as 10% of the beam size, qualified by projected fill patterns for nominal storage ring operation, as an RMS value. For NSLS-II early predictions assumed 80% fill of the storage ring. Experiments at ALS with 500mA dual-cam shaft bunches were a close representation of expected NSLS-II storage ring performance, scaled by the ring circumference, which closely compared with the NSLS-II booster.

Stability for synchrotrons is typically defined over time scales of 8 to 24 hrs, and qualified by the Fast Orbit Feedback (FOFB) bandwidth, often 2KHz for 3rd genera-

*Work supported by DOE contract No: DE-AC02-98CH10886

[#]vetterkg@ornl.gov

tion light sources. The NSLS-II EBPM design objective was to achieve 200nm RMS over an 8hr duration.

Spatial Resolution and Signal-to-Noise Ratio

An estimate of the SNR required to achieve a given spatial resolution can be approximated by [5]

$$\sigma = \frac{\text{aperture}}{2 \cdot \sqrt{2}} \cdot \frac{1}{\sqrt{\text{SNR}}} \tag{1}$$

considering the aperture in (1) to be the horizontal dimension of the NSLS-II large aperture BPM pickup (Fig. 1) of 75mm, the corresponding SNR is 102dB.

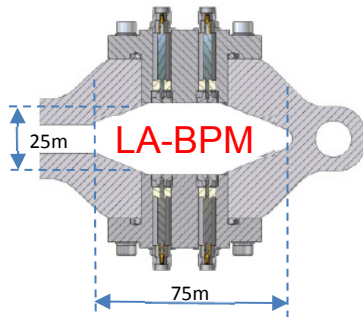


Figure 1: NSLS-II Large Aperture BPM.

This is considered as the intrinsic resolution obtained at the button assuming only Gaussian noise.

Mapping Required SNR into Receiver Dynamic Range

Once an estimate of the required SNR is obtained, it is necessary to being exploration of receiver architectures to determine the optimal SNR mapping to the physical design. Consideration must be given to RF frequency being processed, RF bandwidth, input noise level, and ADC technology.

The NSLS-II EBPM design RF bandwidth is 20MHz which has a single-bunch impulse response of approximately 300ns in duration. A sub-sampling architecture was chosen that directly samples the 500MHz RF signal, stretched to 300ns by the BPF. The LTC2208 16b 125Msps ADC was chosen that yielded 9.9 ENOBs or approximately 60dB of instantaneous SNR [6]. It is necessary to achieve a minimum of 42dB of processing gain, in the defined 2KHz FOFB bandwidth to meet the required 200nm RMS resolution.

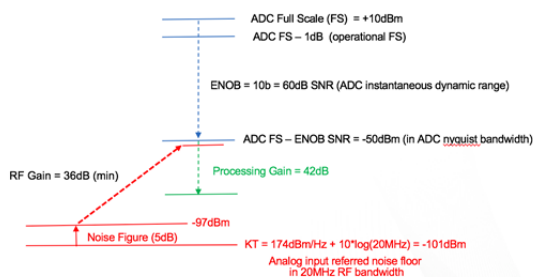


Figure 2: Mapping of required SNR into EBPM receiver.

The mapping of the required SNR into the physical receiver architecture is illustrated in Fig. 2. Assuming a full-scale ADC voltage of 1vp (+10dBm, 50 ohms) provides a reference for the SNR mapping. Subtracting the measured ENOB SNR of 60dB sets the ADC Nyquist noise floor at -50dBm. Next an examination of the receiver noise floor is calculated to be -101dBm for a the specified 20MHz RF bandwidth. An estimation of receiver noise figure of 5dB is derived from nominal cable length using LMR-400 coax, and loss incurred by input BPF. The receiver input referred noise is then calculated to be -97dBm.

To achieve optimal performance as defined by maximizing resolution of low charge single bunch signals to high intensity 500mA 80% stored beam requires mapping of the receiver input referred thermal noise floor to the ADC noise floor by application of appropriate RF gain, and flexibility to attenuate high level signals to prevent ADC saturation, achieving an approximate 90dB receiver dynamic range, without consideration of processing gain.

Receiver Design to Achieve Required Spatial Resolution

The previous sections defined receiver characteristics necessary to achieve the required 200nm in terms of SNR, noise figure, gain and ADC performance. Choice of a sub-sampling receiver topology implies the technology limiting element will be the ADC. Since many ADC data sheets do not include performance for sub-sampling it was necessary to conduct a laboratory analysis. The results of analyzing seven candidate ADCs are shown in Fig. 3. The LTC2208 was selected based on the composite performance of metrics quantified, in particular 3rd order distortion and DC level. The discrete numbers on the plot indicate the measured ENOB for each ADC.

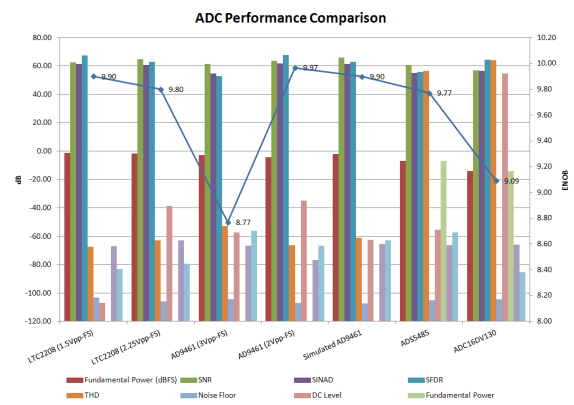


Figure 3: 500MHz ADC sub-sampling performance analysis.

The gain was selected based on SNR defined in previous section in combination with losses of selected receiver components (Fig. 4). The linearity of the receiver design was set to achieve a P1dB of +19dBm and IP3 of +43dBm at the ADC input. The receiver noise figure was set to 5.3dB, primarily driven by the insertion loss of the first SAW BPF. Each channel incorporated a programmable attenuator with a 31dB range and resolution of 1dB

per step to accommodate the required 90dB of dynamic range required to process low charge single bunch TbT signals to high current multi-bunch signals.

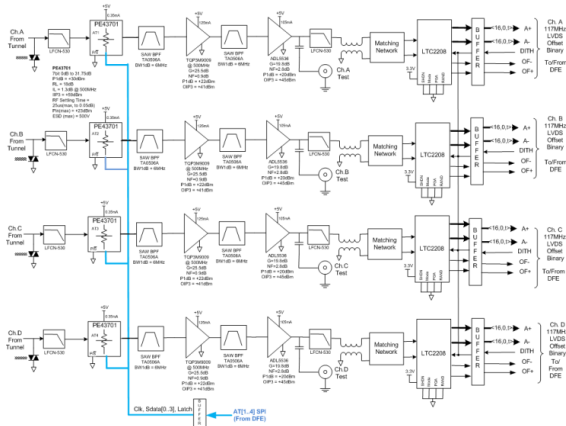


Figure 4: NSLS-II EBPM receiver design.

A sub-miniature connector was incorporated onto the AFE to enable S-parameter measurement of the receiver chain. The full 2x2 S-parameter matrix for a receiver channel from the input to the ADC input anti-aliasing filter is shown below in Fig. 5.

The most critical aspect of the receiver is the ADC. It is important to pay careful attention to the both the RF signal input, and the sampling clock. The differential drive to the ADC was achieved using a microstrip balun that is able to achieve < 1° differential phase balance. Maintaining precise phase balance at the ADC input is important to minimize harmonic distortion induced by ADC.

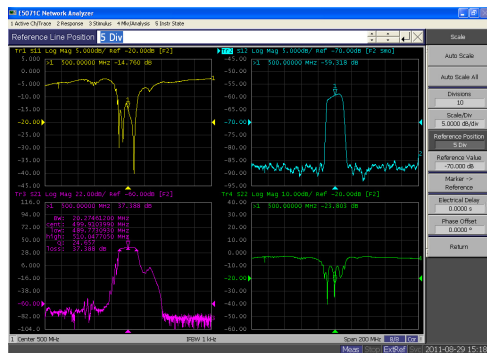


Figure 5: NSLS-II EBPM receiver S-parameters.

The second aspect of importance is to maintain low phase noise at the ADC sampling aperture. This is achieved by incorporating a phased-lock loop (PLL) utilizing the AD9510. The storage ring 378KHz machine clock (499.68MHz / 1320) is distributed to each EBPM and serves as the reference PLL. A balun was incorporated on a spare PLL output to enable measurement of jitter at the ADC sampling aperture which has been quantified to be 700fs from 1Hz – 1MHz.

Optimal Coherent Sampling Numerology

An optimal sampling numerology is then derived based on a receiver topology incorporating precise phase coherence of the ADC sampling clock with respect to the master RF source. The 310th revolution harmonic (117.35MHz) was selected as optimal since it provided sampling numerology compliant with ADC performance, and allowed to have the same PLL VCXO for both the storage ring and booster. The tuning range of the VCXO was defined as +/-100ppm to accommodate the range of the RF master oscillator required for operation and beam experiments, as well as crystal aging of the VCXO estimated to be +/-59ppm.

Periodic sampling produces harmonics of the sampling frequency. Sub-sampling is realized by the difference frequency created by the difference in the 499.68MHz RF beam frequency and the 4th harmonic of the sampling frequency. This frequency corresponds to the 80th harmonic of the revolution frequency or 30.28MHz. Sub-sampling translates the RF signal in the 9th Nyquist zone of the ADC into 1st Nyquist zone.

Phase coherence coupled with a sampling numerology that exhibits integer relationships between the sampling frequency and RF frequency is considered as coherent sampling. The integer relationship translates to an integer number of samples per temporal cycle. Advantages of coherent sampling in the frequency domain is realized by the energy of the RF signal being total contained within a single FFT bin.

The NSLS-II EBPM digital signal processing (DSP) has been developed to exploit coherent frequency domain signal processing. The DSP engine within the FPGA performs position computations based on TbT processing.

Standard DFT based processing for each turn is employed followed by block averaging. The DFT equation based on NSLS-II EBPM numerology is given in (2). A circulating bunch will generate a periodic beam spectrum with frequency domain line spacing equal to the revolution frequency, dependent on the fill pattern. The periodic lines can be considered redundant information so it is in principal necessary to process only a single FFT harmonic to derive an estimate of position. The TbT DFT processing equations are provided below (2-4).

$$X[h_{IF}] = \sum_{n=0}^{h_{Sample}-1} x[n] \cdot W_{h_{Sample}}^{h_{IF} \cdot n} \quad (2)$$

where,

$$W_{h_{Sample}}^{h_{IF} \cdot n} = e^{-\frac{i \cdot 2\pi \cdot h_{IF} \cdot n}{h_{Sample}}} \quad (3)$$

$$X[h_{IF}] = \sum_{n=0}^{h_{Sample}-1} x[n] \cdot e^{-\frac{i \cdot 2\pi \cdot h_{IF} \cdot n}{h_{Sample}}} \quad (4)$$

Equation (4) represents the DFT of the 80th revolution harmonic based on accumulation of 310 samples (1 turn). Subsequent block averaging this DFT coefficient 38-times yields the FOFB 2KHz position estimate.

Single bin DFT coherent performance is shown below in Fig. 6 for a sinewave test tone.

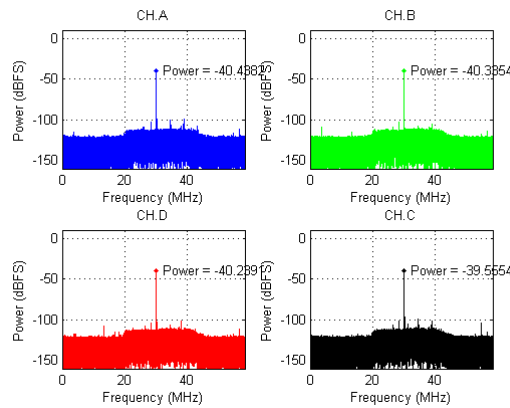


Figure 6: Test tone DFT (1M samples).

A histogram of the test tone is shown in Fig. 7 where the discrete structure is a result of coherent sampling, sampling at exactly the same phase of the sinewave each period of the sinewave.

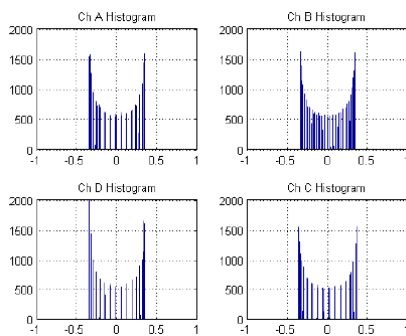


Figure 7: Histogram of sinewave test-tone.

Design for Stability – Pilot Tone

The NSLS-II EBPM was initially developed to utilize an in-band pilot tone to perform periodic calibration corrections. Laboratory long-term stability tests of 19 EBPMs demonstrated sub 200nm RMS stability with rack thermal regulation of 0.01°C RMS. The achievement of long-term stability based solely on thermal stability provided the benefit of beam position measurement without any spectral perturbations. Subsequent in-situ EPBM noise measurements via combiner/splitter confirmed 200nm RMS EBPM stability. Current NSLS-II operations does not employ active pilot tone correction. The pilot tone generator and combiner is used to inject test tones synthesized within the EBPM to perform end-to-end system tests.

Design for Stability – Thermal Electric Regulation

In an attempt to mitigate rack temperature regulation failure influence on EBPM stability, and use of EBPM without precision controlled racks, an experiment was conducted with a thermal electric cooler (TEC) feedback regulation. An experimental setup was constructed utilizing a single TEC per 2-channels resulting in 400nm RMS

stability for a 35hr duration with an ambient temperature variation of 8°C *pp* variation.

The promising results realized from crude experimentations suggests that there is significant room for improvement. A detailed thermal analysis of the RF board enable optimal placement of temperature sensors and TECs, and number of independent control loops would be an interesting R&D activity. There is a significant body of literature on the use of TECs to provide precise thermal control, including TECs embedded in semiconductor lasers.

EBPM OPERATIONAL PERFORMANCE

Resolution

The benefit of coherent sampling frequency domain DFT processing was further improved by adding multiple revolution harmonics within the RF 20MHz passband. Results were first reported by G. Portmann [7] for dual-cam 500mA ALS user beam (Fig. 8).

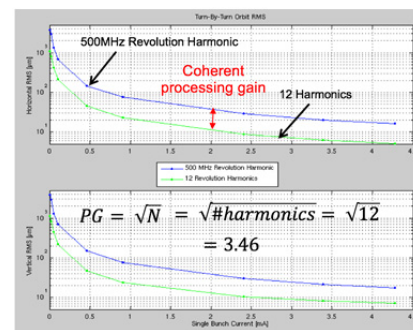


Figure 8: Single Bunch TbT coherent DFT processing gain. ALS dual-cam 500mA user beam.

Recent experiments on NSLS-II by B.Podobedov [4] confirmed coherent TbT DFT processing gain initially reported [3]. Single bunch resolution of about one micron was achieved for ~1 nC/bunch. Multi-bunch 200nm resolution has been demonstrated for 10mA beam (Fig. 9) [2].

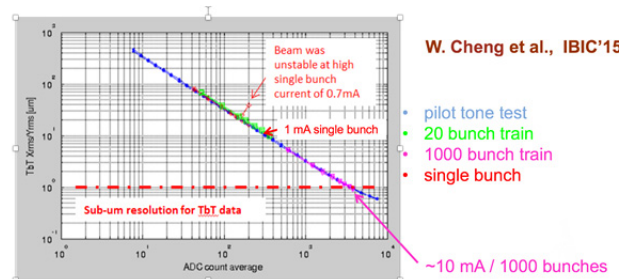


Figure 9: NSLS-II EBPM Resolution.

Orbit Stability

Stability measurements at NSLS-II with active FOFB enabled have demonstrated integrated PSD in the horizontal plane of 800nm (1% of beam size), and 550nm in the vertical plane (10% of beam size), with noise suppression to 250Hz [8]. Measurements are shown in (Fig. 10,11).

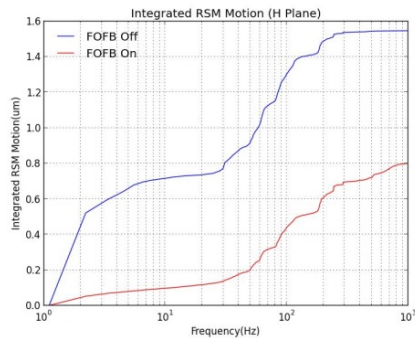


Figure 10: NSLS-II FOFB integrated horizontal PSD performance, noise correction to 250Hz, data collected over 24hrs.

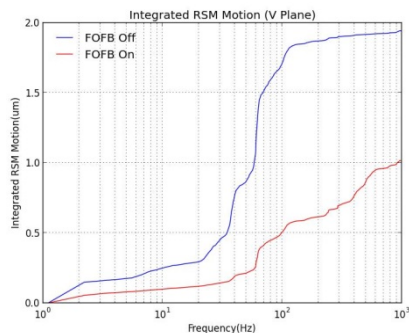


Figure 11: NSLS-II FOFB integrated vertical PSD performance, noise correction to 250Hz, data collected over 24hrs.

DERIVATIVE INSTRUMENTS

The intentional partitioning of the AFE and DFE has led to a suite of derivative instruments including the NSLS-II Cell Controller, Xray BPM based on electrometer AFE, a Diamond BPM also with electrometer based AFE for measurement of photon beam position immediately in front of test sample with feedback servo for monochromator feedback stabilization [9], and LBNL EBPM.

CONCLUSION

A custom EBPM developed at BNL has been successfully commissioned at NSLS-II. Coherent frequency domain digital signal processing has enabled single bunch resolution of 1um for 1nC/bunch. Precision phase coherence has enabled true turn-by-turn measurement capabilities without adjacent turn leakage of signal energy.

The generic architecture with dedicated signal processing board (DFE) and dedicated RF processing board (AFE) has led to the realization of a suite of four derivative instruments have been developed and successfully deployed.

ACKNOWLEDGMENTS

We would like to thank Om Singh for championing the EBPM development project and Ferdinand Willeke for having confidence in the team to re-baseline project to include NSLS-II EBPM.

6: Accelerator Systems: Beam Instrumentation, Controls, Feedback, and Operational Aspects

T03 - Beam Diagnostics and Instrumentation

REFERENCES

- [1] K. Vetter *et al.*, “NSLS-II RF Beam Position Monitor Update,” BIW’2012, pp. 238-241.
- [2] W. Cheng *et al.*, “Characterization of NSLS2 Storage Ring Beam Orbit Stability,” IBIC’2015, pp. 625-629.
- [3] J. Mead *et al.*, “NSLS-II RF Beam Position Monitor Commissioning Update,” IBIC’2014, pp. 500-504.
- [4] B.Podobedov *et.al.*, “Novel Accelerator Physics Measurements Enabled by NSLS-II RF BPM Receivers,” IBIC16.
- [5] S.Smith, “Beam Position Monitor Engineering,” SLAC-PUB-7244, 1996, pp. 11.
- [6] K. Vetter *et al.*, “NSLS-II RF Beam Position Monitor,” PAC’2011, pp. 495-497.
- [7] G. Portmann, private communications, 2010-2012.
- [8] K.Ha *et al.*, “Commissioning of the National Synchrotron Light Source II (NSLS-II) Fast Orbit Feedback System,” ICALEPCS 2015.
- [9] Sydor Technologies <http://sydortechologies.com/>